Research

Cell Calcium (2000) **28** (4), 213–223

doi: 10.1054/ceca.2000.0152, available online at http://www.idealibrary.com on IDEAL®

A comparison of fluorescent Ca^{2+} indicator properties and their use in measuring elementary and global Ca^{2+} signals

D. Thomas[1], S.C. Tovey[1], T.J. Collins,[1] M.D. Bootman[1,2], M. J. Berridge,[1,2] P. Lipp[1]

[1]Laboratory of Molecular Signalling, The Babraham Institute, Babraham, Cambridge, UK
[2]Department of Zoology, University of Cambridge, Cambridge, UK

Summary Quantifying the magnitude of Ca^{2+} signals from changes in the emission of fluorescent indicators relies on assumptions about the indicator behaviour in situ. Factors such as osmolarity, pH, ionic strength and protein environment can affect indicator properties making it advantageous to calibrate indicators within the required cellular or subcellular environment. Selecting Ca^{2+} indicators appropriate for a particular application depends upon several considerations including Ca^{2+} binding affinity, dynamic range and ease of loading. These factors are usually best determined empirically. This study describes the in-situ calibration of a number of frequently used fluorescent Ca^{2+} indicators (Fluo-3, Fluo-4, Calcium Green-1, Calcium Orange, Oregon Green 488 BAPTA-1 and Fura-Red) and their use in reporting low- and high-amplitude Ca^{2+} signals in HeLa cells. All Ca^{2+} indicators exhibited lower in-situ Ca^{2+} binding affinities than suggested by previously published in-vitro determinations. Furthermore, for some of the indicators, there were significant differences in the apparent Ca^{2+} binding affinities between nuclear and cytoplasmic compartments. Variation between indicators was also found in their dynamic ranges, compartmentalization, leakage and photostability. Overall, Fluo-3 proved to be the generally most applicable Ca^{2+} indicator, since it displayed a large dynamic range, low compartmentalization and an appropriate apparent Ca^{2+} binding affinity. However, it was more susceptible to photobleaching than many of the other Ca^{2+} indicators.

INTRODUCTION

The calcium ion, Ca^{2+}, is an intracellular messenger capable of controlling a diverse range of cellular processes and has its major signalling function during spatiotemporally complex elevations in the cytoplasmic compartment of the cell [1,2]. At the lowest level, Ca^{2+} signalling comprises spatially restricted 'elementary' Ca^{2+} signals, whilst summation of elementary signals can construct larger 'global' Ca^{2+} signals that invade the entire cell [3,4]. Observation of these signals has been made possible using fluorescent Ca^{2+} indicators that change their light absorption and/or emission characteristics upon Ca^{2+} binding.

A large number of fluorescent Ca^{2+} indicators are available for studying Ca^{2+} in cells [5]. Most are based on the Ca^{2+} chelators EGTA or BAPTA modified to incorporate fluorescent reporter groups [6,7]. In conjunction with these Ca^{2+} indicators, development of confocal and fluorescence microscopy enabled us to visualize rapid Ca^{2+} fluctuations in subcellular volumes. However, care must be taken in calculating Ca^{2+} concentrations from raw fluorescence levels. The most straightforward solution for converting fluorescence into Ca^{2+} concentrations is to determine in-situ calibration curves. Such curves account for the effects of the cellular environment on the

Received 26 July 2000
Accepted 27 August 2000

Correspondence to: Martin D. Bootman, Laboratory of Molecular Signalling, The Babraham Institute, Babraham, Cambridge CB2 4AT, UK.
Tel.: +44 (0) 1223 496 515; Fax: 01223 496 033;
E-mail: martin.bootman@bbsrc.ac.uk

Table 1 Composition of experimental solutions

	HeLa buffers (mM)		Calibration buffers (mM)	
Compound	Control	Modified	CaEGTA	EGTA
NaCl	121.0	121.0	121.0	121.0
KCl	5.4	5.4	5.4	5.4
$MgCl_2$	0.8	0.8	0.8	0.8
$CaCl_2$	1.8	1.8	4.0	–
$NaHCO_3$	6.0	6.0	6.0	6.0
D-glucose	5.5	–	–	–
HEPES	25.0	25.0	25.0	25.0
2-deoxy-D-glucose	–	1.8	1.8	1.8
EGTA	–	–	4.0	4.0
Rotenone	–	0.01	0.01	0.01
A23187	–	0.01	0.01	0.01
pH	7.30 ± 0.01	7.30 ± 0.01	7.30 ± 0.01	7.30 ± 0.01

characteristics of an indicator. Furthermore, if spatial resolution permits, the properties of an indicator can be measured in different cellular compartments.

The present study describes an empirical assessment of the properties and usefulness of the most commonly-used visible-wavelength fluorescent Ca^{2+} indicators (Fluo-3, Fluo-4, Calcium Green-1, Calcium Orange, Oregon Green 488 BAPTA-1 and Fura-Red). The affinities of these indicators for Ca^{2+} in the cytosolic and nuclear compartment of HeLa cells were determined. Other features of these indicators, such as their resistance to photobleaching and propensity to compartmentalize, were also monitored. Most of the indicators had some characteristics that enhanced their usefulness, but no one indicator provided an ideal combination of properties.

MATERIALS AND METHODS

Cell culture

HeLa cells (ATCC, CCL-2) were cultured in sterile flasks with Eagles minimum essential medium containing: glutamine (2 mM), penicillin (55 units/ml), streptomycin (55 mg/ml), and serum (5% v/v of a 1:1 foetal:newborn bovine mixture). Cells were incubated in a humid atmosphere (5% O_2:95% CO_2; 37°C), media replaced every other day, and cells passaged at ~80% confluence. In preparation for experiments, cells were plated onto glass coverslips and returned to the incubator for 24–48 h to ensure adequate adhesion. Prior to experiments, the culture medium was removed. The coverslips were washed with control HeLa buffer (see Table 1), placed in sandwich chambers and mounted on the stage of a confocal laser scanning microscope [8].

Loading, compartmentalization, leakage and photobleaching of fluorescent Ca^{2+} indicators

Stock solutions (1 mM) of the AM-ester form of all fluorescent Ca^{2+} indicators were made using a solution of 20% (w/v) Pluronic F-127 in absolute dimethylsulphoxide (DMSO). Aliquots were diluted with unmodified HeLa buffer to give final concentrations of: Fluo-3, 2 μM; Fluo-4, 1 μM; Calcium Green-1, 2 μM; Calcium Orange, 2 μM; Oregon Green 488 BAPTA-1, 2 μM; and Fura-Red, 2 μM. Cells were loaded with the fluorescent Ca^{2+} indicators for 30 mins, washed in unmodified HeLa Buffer, and left for a further 30 mins to allow de-esterification. These concentrations were determined empirically and provided sufficient loading for visualization of Ca^{2+} signals [9].

Compartmentalization and leakage of the Ca^{2+} indicators were assessed using high resolution images obtained on a PerkinElmer Life Sciences UltraView confocal microscope. Cells were loaded with fluorescent indicators as described above, and incubated for 30 mins at either room temperature (20–22°C) or 37°C before the subcellular distribution of fluorescent indicators was examined.

Photobleaching of Ca^{2+} indicators was quantified by determining the rate at which the fluorescent signal declined during 30 min of constant illumination on a NORAN *Oz* confocal microscope with the intensity of excitation light at the objective aperture set to 20 μW (determined using a Coherent Lasercheck power meter). Images of 1 s duration were captured every 5 s (320 × 240 pixels at 7.5 Hz, jump average of 4 frames, optical section ~1.5 μm). Fluorescence traces were fitted using a non-linear least squares algorithm to $f = f_0 e^{-(kt)}$ where f_0 is the initial fluoresence, t represents a given moment in time and k is the decay constant. The half-life of the fluorescence signal was determined using $t_{1/2} = k^{-1}$.

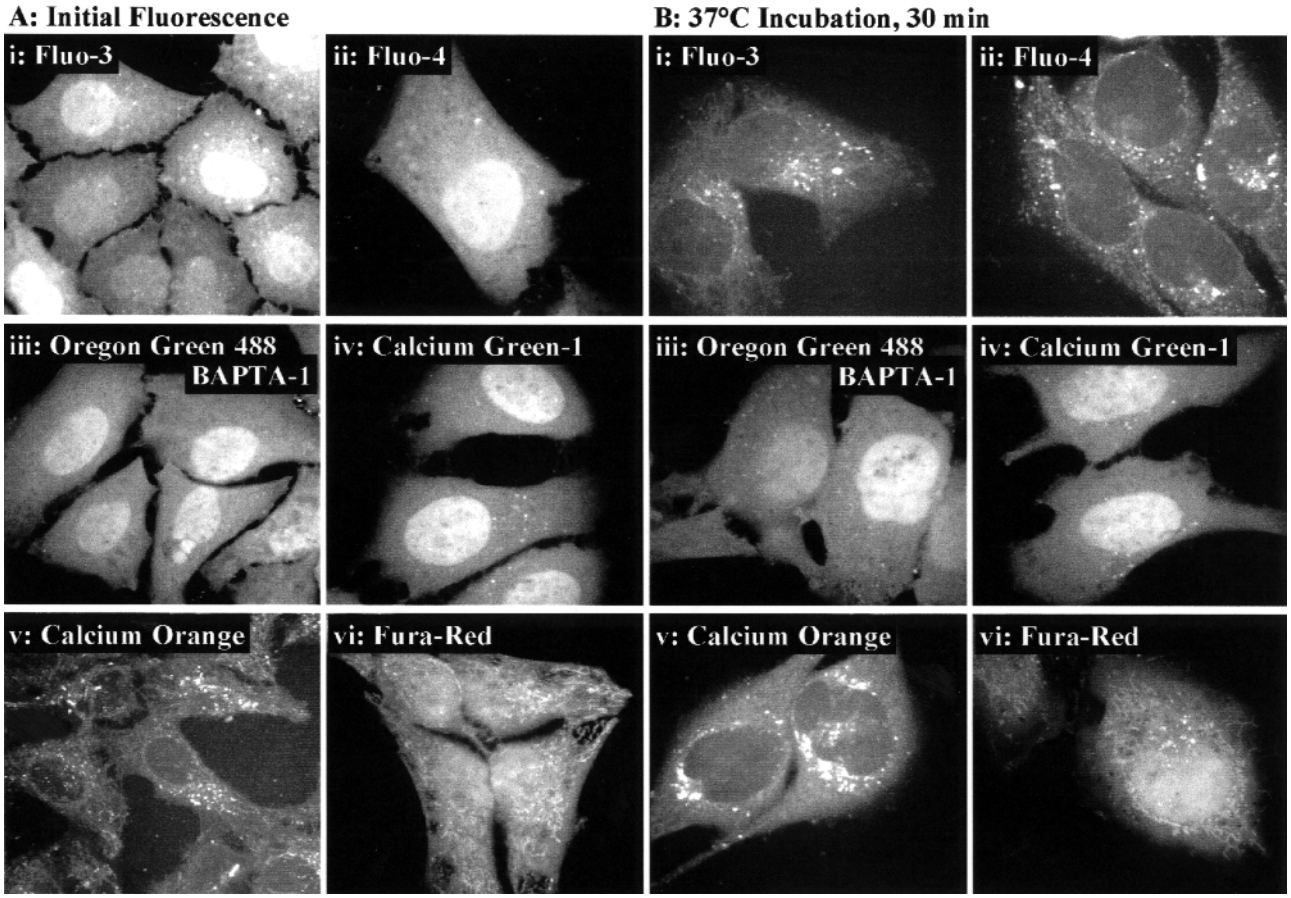

Fig. 1 Loading, compartmentalization and leakage of fluorescent Ca^{2+} indicators. Cells were loaded with fluorescent Ca^{2+} indicators for 30 mins and allowed a further 30 mins for de-esterification. Following this period, cells loaded with (Ai) Fluo-3, (Aii) Fluo-4, (Aiii) Oregon Green 488 BAPTA-1 or (Aiv) Calcium Green-1 displayed a uniform cytoplasmic fluorescence with a higher fluorescent signal from the nucleus. Cells loaded with either (Av) Calcium Orange or (Avi) Fura-Red showed marked mitochondrial/ER compartmentalization. Incubation at 37°C (30 min) results in a marked loss of (Bi) Fluo-3 and (Bii) Fluo-4 fluorescence and revealed an underlying mitochondrial/ER compartmentalization. Fluorescence in (Biii) Oregon Green 488 BAPTA-1 and (Biv) Calcium Green-1-loaded cells remained uniform, whilst (Bv) Calcium Orange and (Bvi) Fura-Red-loaded cells still displayed marked compartmentalization.

In-situ calibration of fluorescent Ca^{2+} indicators

Calibration solutions were made using the method of Bers [10, 11]. Essentially, known quantities of EGTA and CaEGTA solutions (see Table 1 for compositions) were mixed to provide solutions containing different total Ca^{2+} concentrations. Confirmation of the free Ca^{2+} concentration was performed using a Ca^{2+}-sensitive electrode with corrections made for background Ca^{2+} contamination and EGTA impurity [11]. All solutions were adjusted to pH 7.30 ± 0.01 at room temperature.

Cells loaded with the fluorescent Ca^{2+} indicators were permeabilized with A23187 (10 μM), equilibrated in the mixed EGTA/CaEGTA solution (15 min), and fluorescence averaged over 1 s at the end of this period using either a NORAN *Odyssey* or *Oz* confocal microscope running a time-series protocol (320 × 240 pixels at 7.5 Hz, jump average of four frames, optical section ~1.5 μm). Maximum fluorescence was established by exposing cells to a solution with a Ca^{2+} concentration of 2 mM. Minimum fluorescence was obtained after incubating the cells with the EGTA buffer alone. Concentration–response curves were fitted using a non-linear least-squares algorithm to $f=\{(f_{max})/(1 + [K_d/x]^{nH})\}$ where f was the fluorescence intensity, f_{max} was the fluorescence obtained in the presence of 2 mM Ca^{2+}, x was the free Ca^{2+} concentration, nH was the Hill coefficient and K_d was the apparent Ca^{2+} binding affinity.

Suitability of fluorescent Ca^{2+} indicators for recording Ca^{2+} signals

Indicator-loaded cells were mounted on the stage of a NORAN *Odyssey* or *Oz* confocal microscope and fluorescence images captured using a time-series protocol. The cells were continually perfused with unmodified HeLa buffer and local application of histamine (1 μM) was

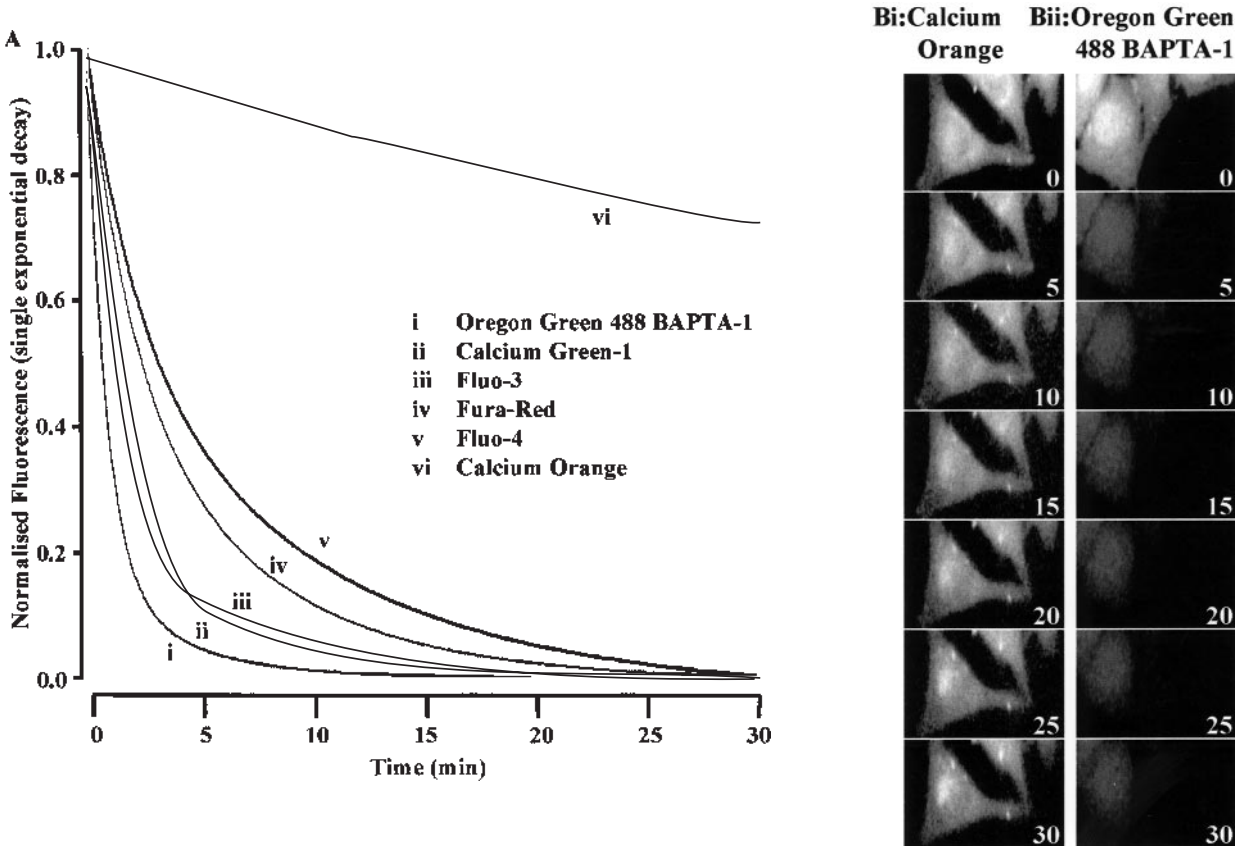

Fig. 2 Photobleaching of fluorescent Ca^{2+} indicators. (A) The time-dependent loss of relative fluorescence during continuous laser illumination (20 μW). The curves were fitted assuming single exponential decays (see text for details). Curves are fitted to the mean data from ≥3 cells loaded with each Ca^{2+} indicator. Time-lapse series of images illustrate the difference in photobleaching between (B i) Calcium Orange and (B ii) Oregon Green 488 BAPTA-1.

achieved by means of a solenoid-driven rapid-switching device ($t_{1/2}$ of mixing ~0.5 s). Our previous studies have shown that this histamine concentration is capable of evoking both elementary Ca^{2+} release events and global Ca^{2+} waves [4,8]. Experimental records were subsequently exported to a modified version of NIH-Image for off-line analysis.

Changes in $[Ca^{2+}]_i$ were calculated using:

$$[Ca^{2+}]_i = K_d\{(f\text{-}f_{min})/(f_{max}\text{-}f)\}$$

where the K_d was the apparent Ca^{2+}-binding affinity of the Ca^{2+} indicator determined *in situ*, f_{min} and f_{max} were the minimum and maximum fluorescence intensities determined with EGTA or 2 mM Ca^{2+} solutions (see above), and f was the fluorescent intensity at any given time point. Spatially restricted increases in Ca^{2+} concentration were considered as being genuine elementary events if they met previously described criteria [8]. Essentially, the peak amplitude of an event had to be achieved within three frames (i.e. ~400 ms) and be greater than twice the standard deviation of the basal Ca^{2+} fluctuation.

RESULTS AND DISCUSSION

Loading, compartmentalization, leakage and photobleaching of fluorescent Ca^{2+} indicators

Ca^{2+} indicators are membrane impermeant in their Ca^{2+}-sensitive form, and AM-ester linkage provides a convenient method for introducing indicators into cells. AM-ester groups are cleaved by endogenous esterases thus releasing the Ca^{2+}-sensitive form of the indicator intracellularly. However, the esterified Ca^{2+} indicators can also cross other cellular membranes, such as those of intracellular organelles, where esterase activity results in their compartmentalization. In addition to this passive compartmentalization, cells can actively compartmentalize the acid form of indicators from the cytosol into subcellular compartments [12].

HeLa cells loaded with Oregon Green 488 BAPTA-1 generally displayed uniform cellular fluorescence patterns, without obvious accumulation in subcellular organelles (Fig. 1A). At the other extreme, cells loaded with either Calcium Orange or Fura-Red consistently displayed marked mitochondrial and/or endoplasmic

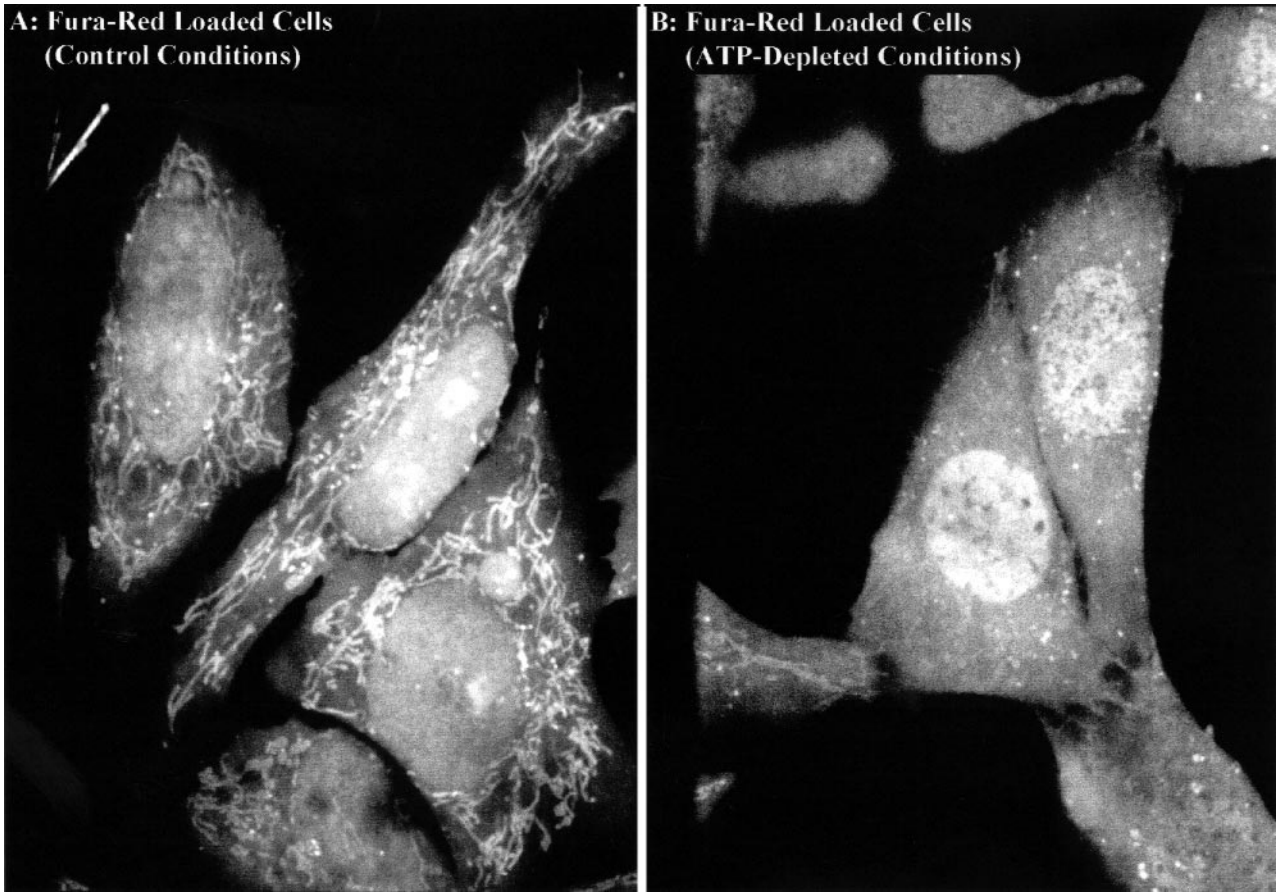

Fig. 3 Effect of ATP-depletion on Ca^{2+} indicator compartmentalization. (A) Fura-Red-loaded cells display marked compartmentalization when indicator loading was carried out under normal experimental conditions. In order to achieve accurate calibration of the Ca^{2+} indicators compartmentalization had to be prevented. (B) Depletion of cellular ATP levels with the mitochondrial inhibitor rotenone (10 μM) and replacement of glucose with 2-deoxy-D-glucose prevented compartmentalization of the Ca^{2+} indicators and resulted in a more uniform cytoplasmic and nuclear fluorescence. Similar results were seen with Calcium Orange, which also showed marked compartmentalization under normal experimental conditions (not shown).

reticulum (ER) compartmentalization (Figs 1Av–vi). Furthermore, Calcium Orange-loaded cells always contained large numbers of highly fluorescent perinuclear vesicles (Fig. 1Av). Fluo-3-, Fluo-4- and Calcium Green-1-loaded cells tended to show a uniform cytoplasmic fluorescence (Figs 1Ai, ii & iv), although mitochondrial/ER staining was seen in a minority of cells. The nuclei of cells loaded with Fluo-3, Fluo-4, Fura-Red, Oregon Green 488 BAPTA-1 or Calcium Green-1 possessed a higher fluorescence than that of the surrounding cytoplasm (Figs 1Ai-iv & vi). In contrast, the nuclei of Calcium Orange-loaded cells was less fluorescent than the cytosol (Fig. 1Av), suggesting that substantial amounts of Calcium Orange became compartmentalized.

Although the de-esterified Ca^{2+}-indicators are effectively membrane impermeant and unable to leave cells by diffusion, anion transporters present in the plasma membrane can cause the clearance of indicators. These transporters are temperature sensitive, hence, experimental temperature can impact on the rate of indicator loss. Cells loaded with fluorescent Ca^{2+} indicators and left at room temperature (20–22°C) for 30 mins showed little difference in fluorescence compared to freshly loaded cells (not shown). However, incubation of Fluo-3- or Fluo-4-loaded cells at 37°C resulted in a dramatic loss of cytoplasmic fluorescence, and revealed the underlying mitochondrial/ER compartmentalization (Figs 1Bi–ii). These cells typically exhibited the highly

Table 2 Photodestruction of fluorescent Ca^{2+}-indicators

Ca^{2+}-indicator	Exponential decay $t_{1/2}$(S)
Fluo-3	143
Fluo-4	339
Calcium Green-1	123
Oregon Green 488 BAPTA-1	73
Calcium Orange	2441
Fura-Red	251

Data is expressed as the half-lives of curves fitted to the mean of at least three separate determinations of the rate of photobleaching.

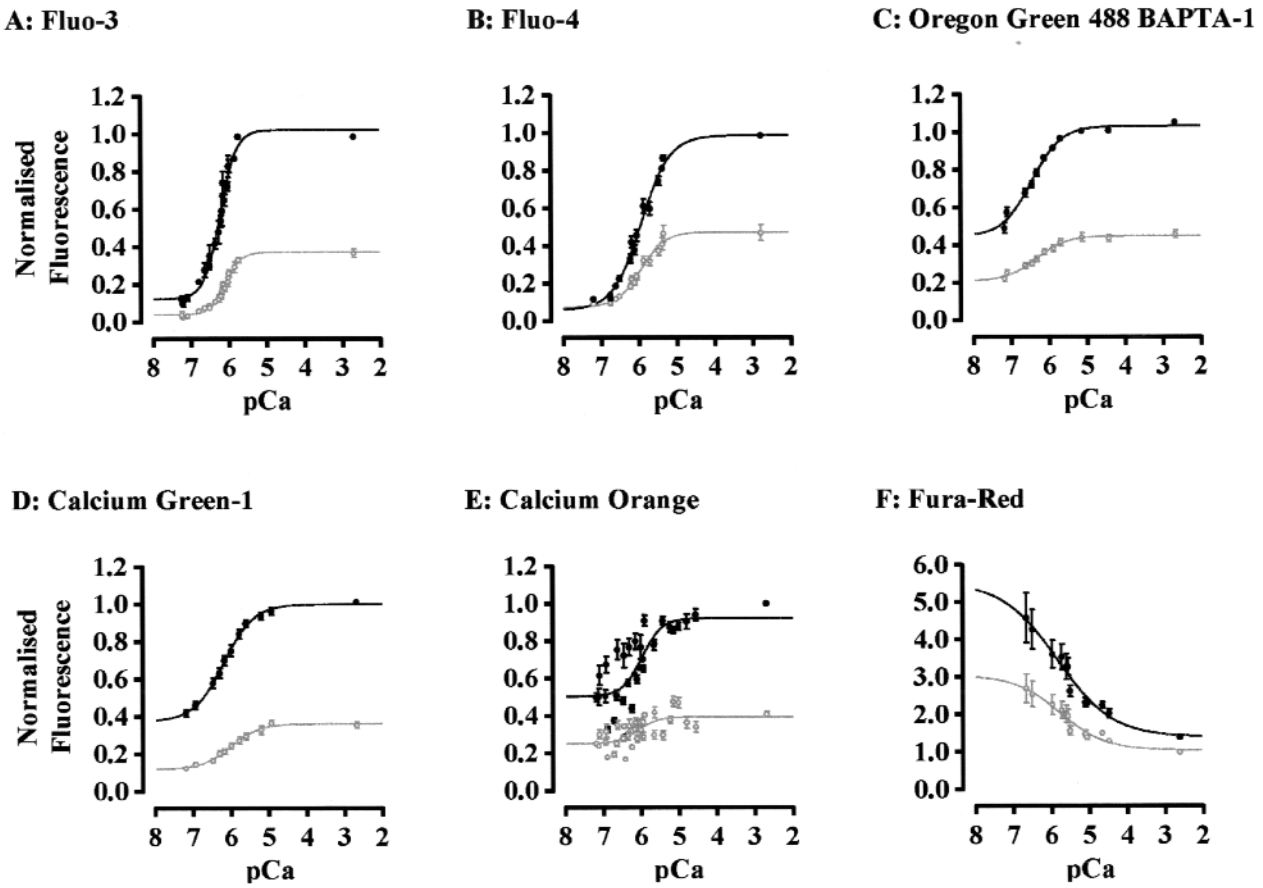

Fig. 4 In-situ calibration of fluorescent Ca^{2+}-indicators. EGTA/CaEGTA solutions were used to construct concentration response curves illustrating the in situ Ca^{2+}-dependent fluorescence of (A) Fluo-3, (B) Fluo-4, (C) Oregon Green 488 BAPTA-1, (D) Calcium Green-1 (E) Calcium Orange and (F) Fura-Red. Black and grey data points represent the nuclear and cytoplasmic fluorescence respectively. The data points are the mean ± SEM of ≥11 cells for each Ca^{2+} indicator.

Table 3 In-situ properties of fluorescent Ca^{2+}-indicators.

	Apparent Ca^{2+}-binding (nM)			Dynamic Range		Hill Coefficient		
Ca^{2+}-indicator	In vitro§	Cytoplasmic	Nucleoplasmic	Cytoplasmic	Nucleoplasmic	Cytoplasmic	Nucleoplasmic	*n*
Fluo-3	390	810 ± 50	620 ± 45*	7.7	7.9	2.2	1.9	16
Fluo-4	345	1000 ± 130	1260 ± 160	6.0	15.0	1.4	1.1	11
Calcium Green-1	190	930 ± 90	600 ± 50	2.8	3.5	1.1	1.1	22
Oregon Green 488 BAPTA-1	170	430 ± 80	320 ± 60	2.6	2.5	1.1	1.1	24
Calcium Orange	185	1100 ± 400	1600 ± 500	1.6	2.1	1.2	0.8	14
Fura-Red	140	650 ± 55	690 ± 80	3.8	4.2	1.4	1.3	14

Apparent Ca^{2+}-binding affinity is expressed as mean ± sem of n cells, Dynamic Range and Hill Coefficients taken from the curves fitted to the mean data from *n* cells (see Fig. 4).
§Ca^{2+}-binding affinity determined by manufacturer [5].
* Compartment in which a significantly higher apparent Ca^{2+}-binding affinity was observed.

fluorescent perinuclear vesicles observed in cells loaded with Calcium Orange at room temperature (Fig. 1Av). The pattern of fluorescence in cells loaded with either Fura Red, Calcium Orange, Oregon Green 488 BAPTA-1 or Calcium Green-1 was broadly similar before and after incubation at 37°C; Fura-Red- and Calcium-Orange-loaded cells still had marked compartmentalization (Figs 1Bv–vi), whilst Calcium-Green-1- and

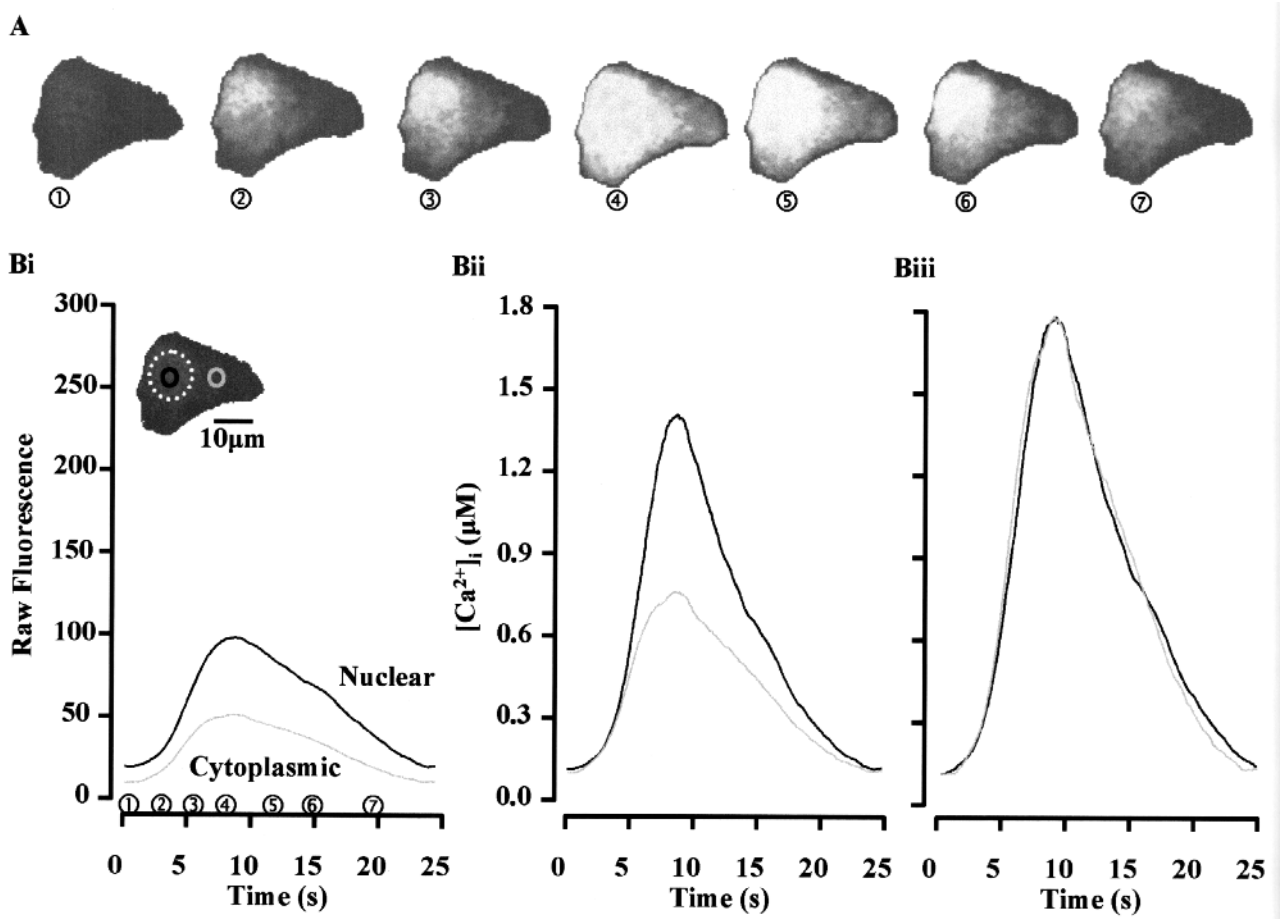

Fig. 5 Artifactual Ca^{2+} gradients between the nucleus and cytoplasm. (A) A montage of images showing the passage of a histamine-evoked Ca^{2+} wave across a HeLa cell and (Bi) the corresponding increase of nuclear (black trace) and cytoplasmic (grey trace) fluorescence. The data were obtained by averaging the fluorescence emission from the regions marked on the cell image in Bi. The dotted circle represents the position of the nucleus. Calibration of the raw fluorescence using (Bii) a self ratio against basal fluorescence, an assumed K_d of 500 nM and a dynamic range of 6, gives the impression of a sustained Ca^{2+} gradient between the nuclear and the cytoplasmic compartments. However, this gradient is not apparent (Biii) if the data are calibrated using the Ca^{2+} indicator properties derived from the in-situ calibration.

Oregon Green 488 BAPTA-1-loaded cells retained uniform cytoplasmic fluorescence (Figs 1Biii–iv). These results suggest that for different indicators their concentration ratio between cytosolic and organellar compartments can vary with temperature, and this phenomenon might have to be taken into account when measuring fluorescence from ester-loaded cells.

Photobleaching is the irreversible damage of Ca^{2+}-indicator molecules generating a less fluorescent species and, thus, a decrease of fluorescence signal over time. It should also be noted that indicators might produce highly fluorescent species that are Ca^{2+} insensitive (so-called 'antibleaching'). As a consequence of that, resting fluorescence will increase and the relative fluorescence changes to a given Ca^{2+} will be reduced. The more resistant a Ca^{2+} indicator is to photobleaching, the longer it can provide useful information about the Ca^{2+} signals being imaged. The relative bleach rates of the Ca^{2+} indicators were assessed by continuous exposure of loaded cells to a standardized (20 μW) laser illumination (similar to the energies used in typical confocal imaging experiments). With all indicators, a time-dependent exponential loss in fluorescence was observed (Table 2, Fig. 2). Despite being resistant to clearance/leakage, Oregon Green 488 BAPTA-1 was the most susceptible to photodestruction ($t_{1/2}$ = 73 s). Conversely, those Ca^{2+} indicators for which compartmentalization, clearance or leakage were problematic appeared more resistant, e.g. Fluo-4 and Fura-Red ($t_{1/2}$ = 339 s and 251 s respectively) whilst Fluo-3 and Calcium Green-1 had intermediate rates of photobleaching ($t_{1/2}$ = 143 s and 123 s respectively). In our hands, Calcium Orange is remarkably resistant to photobleaching, and shows considerably less reduction in fluorescence despite continual illumination (Table 2, Fig. 2). This assessment did not take into account the relative brightness of the Ca^{2+} indicators. For

example, Fluo-4 is brighter than Fluo-3, hence during experiments a lower excitation intensity would typically be used for Fluo-4, which would reduce photobleaching.

In-situ calibration of fluorescent Ca^{2+} indicators

Initial attempts to construct calibration curves for the various Ca^{2+} indicators were hampered by the ability of HeLa cells to regulate cytosolic Ca^{2+} to normal levels despite the presence of Ca^{2+} ionophore A23187. Cells were, therefore, depleted of ATP to inhibit Ca^{2+} ATPases using a combination of rotenone (10 μM) and replacement of glucose in the extracellular medium with 2-deoxy-D-glucose. Incubation with these compounds did not affect the morphology of the cells for several hours, but did allow the cytosol to equilibrate with the externally applied Ca^{2+}/EGTA solutions. In addition, ATP depletion prevented compartmentalization of the indicators, including Calcium Orange and Fura-Red (Fig. 3), which were most prone to sequestration.

Mixing EGTA and CaEGTA buffers in ratios 1:3 to 40:1 yielded solutions with a free [Ca^{2+}] range of pCa 7.22 to 2.77 (60 nM to 1.7 mM). Concentration–response curves were obtained from both nuclear and cytoplasmic compartments for all Ca^{2+} indicators (Fig. 4). With each indicator, a shift to lower apparent Ca^{2+}-binding affinities was seen when compared to the in-vitro affinities determined by the manufacturer (Table 3) [5]. The shift in Ca^{2+}-binding affinity ranged from ~1.5-fold for nuclear Fluo-3 through to ~8.5-fold for nuclear Calcium Orange (Table 3). Two of the Ca^{2+} indicators showed significantly different Ca^{2+}-binding affinities between the nuclear and cytoplasmic compartments (Fluo-3, 810 ± 50 nM and 620 ± 45 nM; Calcium Green-1, 930 ± 90 nM and 600 ± 50 nM in the cytoplasmic and nuclear compartments respectively).

Several previous studies using fluorescent Ca^{2+} indicators have suggested that cells display nuclear/cytoplasmic Ca^{2+} gradients [13]. We have not seen a convincing demonstration of such a gradient, and suggest that they may simply arise owing to problems in fluorescent dye calibration. An illustration of an apparent nuclear/cytosolic Ca^{2+} gradient during a cellular Ca^{2+} response, and its correction, are illustrated in Figure 5. In this example, three representations of the same data are displayed. The first simply represents the raw 8-bit data obtained by monitoring fluorescence in the cytosol and nucleus (Figs 5A & Bi). There is a clear difference in the absolute fluorescence levels in the two compartments. Calibrating Ca^{2+} concentrations assuming a K_d of 500 nM and a dynamic range of 6 for both compartments [5] preserves the apparent gradient (Fig. 5Bii). If the nuclear and cytoplasmic Ca^{2+} concentrations are calculated using the properties of the Ca^{2+} indicators determined by the in-situ calibration described herein (see Table 3), then there is no gradient (Fig. 5Biii). Clearly, different processing of the same data yielded markedly different interpretations.

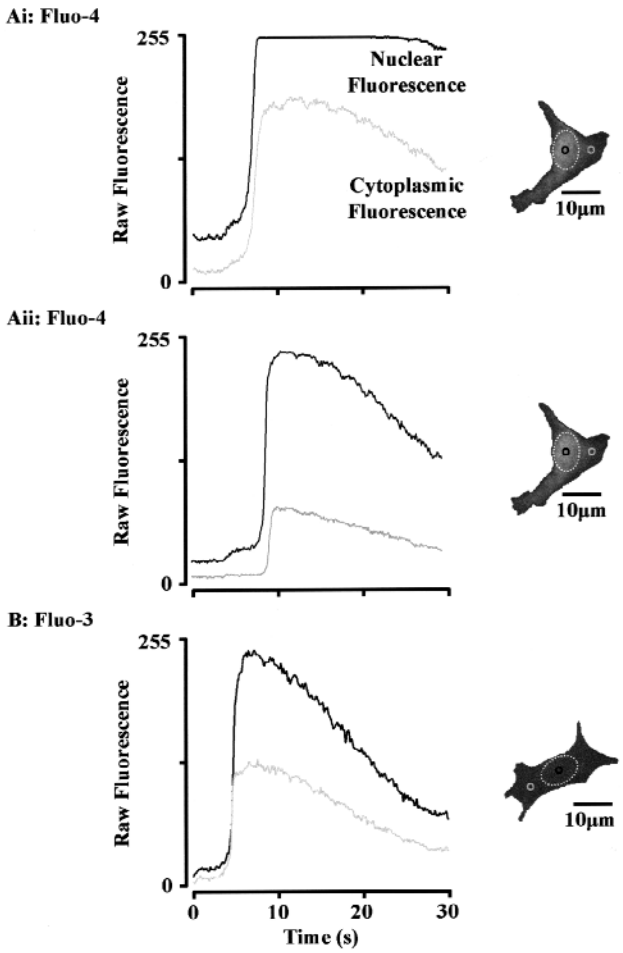

Fig. 6 Detector saturation with high-amplitude Ca^{2+} signals (Ai) Depicts the saturation of the photo multiplier by Fluo-4 in the nucleus of a HeLa cell during a histamine-evoked Ca^{2+} wave. (Aii) Reducing the photo multiplier gain alleviates the saturation and allows the full range of nuclear fluorescence change to be captured, however there is a significant reduction in the number of bits available for monitoring cytoplasmic fluorescence (B) A Fluo-3-loaded cell imaged using the same gain settings as in Ai illustrates that for Fluo-3 a reasonable number of bits is available for monitoring cytoplasmic changes in fluorescence, whilst avoiding the problem of saturating levels of nuclear fluorescence.

The greater brightness of Ca^{2+} indicators in the nuclear compartment poses another problem during Ca^{2+} imaging – that of detector saturation. For all indicators (obviously excepting Fura-Red), global Ca^{2+} signals result in fluorescence increases that are considerably larger in the nucleus than in the cytoplasm. For Fluo-4, which has a dynamic range of 15 in the nuclear compartment, this is a particular problem. If the gain (contrast) settings are adjusted so that the signal from the cytoplasmic Fluo-4 fills the image bit-depth, then the nuclear signal

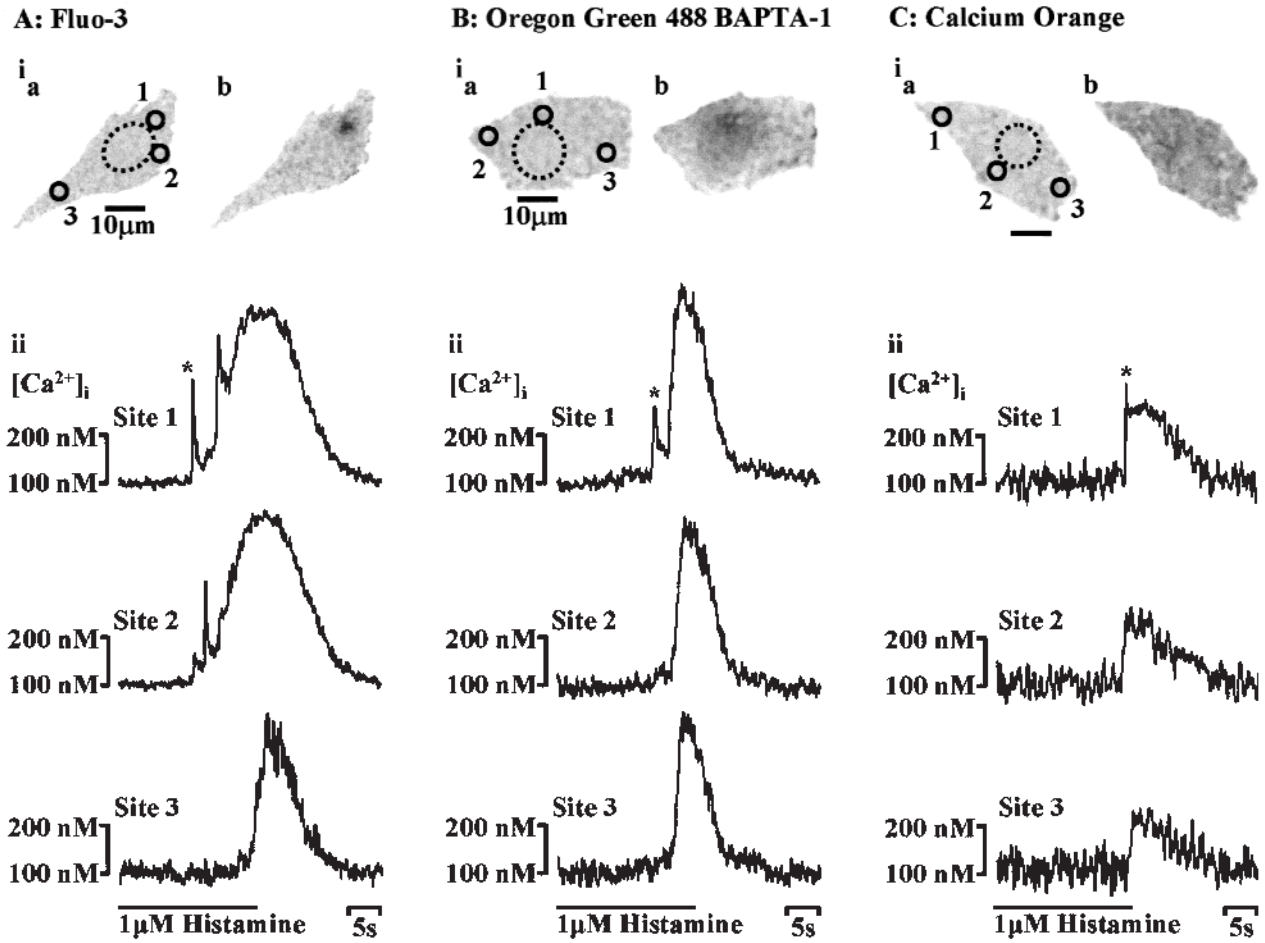

Fig. 7 Visualization of subcellular and global Ca^{2+} signals. HeLa cells loaded with (A) Fluo-3, (B) Oregon Green 488 BAPTA-1 or (C) Calcium Orange and stimulated with histamine (1 μM) reveal the comparative ease with which elementary and global Ca^{2+} signals can be observed using different indicators. Subcellular elementary Ca^{2+} events are clearly visible in those cells loaded with either (A) Fluo-3 or (B) Oregon Green 488 BAPTA-1, whilst only wave initiation points are apparent in (C) Calcium Orange-loaded cells. The traces in panels Aii, Bii and Cii represent the changes in Ca^{2+} observed at the regions indicated in panels Ai_a, Bi_a and Ci_a, whilst the dotted line represents the position of the nucleus. Those Ca^{2+} signals marked with asterisk (*) in panels Aii, Bii and Cii are illustrated in panels Ai_b, Bi_b and Ci_b.

will saturate the detector (Fig. *6*Ai). Reducing the photo multiplier gain prevents saturation, but also substantially decreases the ability and accuracy of detecting small changes in cytoplasmic fluorescence (Fig. *6*Aii). In non-confocal imaging techniques, where the nuclear and cytoplasmic volumes may not be distinguishable, Fluo-4 signals will be dominated by the fluorescence emission from the nucleus. This problem is also apparent with indicators, such as Fluo-3 (Fig. *6*B), but is less serious owing to their smaller nuclear dynamic range (Table 3).

Suitability of fluorescent Ca^{2+}-indicators for recording cellular Ca^{2+} signals

Since many cells produce Ca^{2+} signals ranging from rapid, spatially-restricted, elementary events through to global elevations that invade the whole cell [4,8], it is desirable to use a single indicator that permits reasonable detection of both small and large Ca^{2+} changes. HeLa cells respond to low histamine concentrations with elementary Ca^{2+} signals typically ~15–300 nM, with a spatial spread of ~2–7 μm and a total duration of ~1 s [4]. Higher histamine concentrations produce repetitive global Ca^{2+} waves with amplitudes >500 nM that persist for tens of seconds [14]. During our studies of elementary and global Ca^{2+} signalling, we have examined the suitability of different indicators for monitoring these diverse events.

An illustration of the ease with which different Ca^{2+} indicators can be used to monitor elementary and global Ca^{2+} signals is depicted in Figure 7. In our hands the most versatile indicator by far is Fluo-3 (or Fluo-4). Figure 7A shows an example of elementary and global Ca^{2+} signals detected using Fluo-3. In this example, histamine stimu-

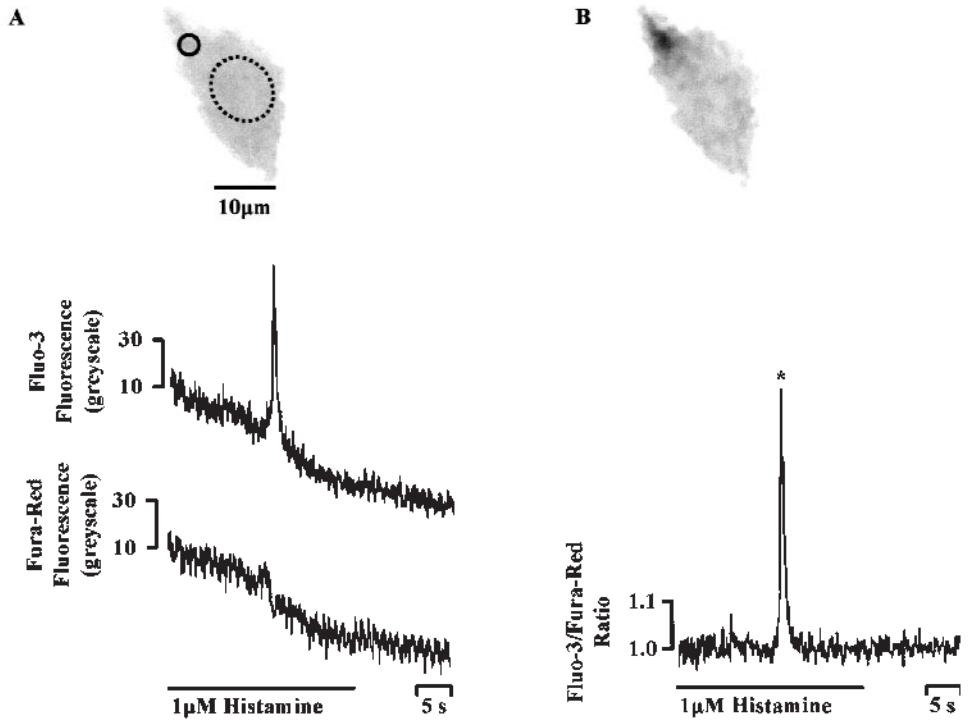

Fig. 8 The combined use of Fluo-3 and Fura-Red for ratiometric Ca^{2+} imaging. (A) A histamine-evoked elementary Ca^{2+} release event recorded in a HeLa cell loaded with both Fluo-3 and Fura-Red. Ca^{2+} release results in an increase in Fluo-3 fluorescence and a corresponding decrease in Fura-Red fluorescence. Note that there is marked photobleaching with both Ca^{2+} indicators. (B) Taking the fluorescence ratio of these two indicators results in a loss of the photobleaching artefact found for the individual dyes and improves the signal-to-noise of the recording. The traces in panels A and B show the fluorescence changes observed in the region marked with the continuous line in the cell image in A, whilst the dotted line indicates the position of the nucleus. The ratiometric cell image in panel B depicts the local Ca^{2+} signal marked with an asterisk (*) in the tracings.

lation initially evoked an elementary Ca^{2+} release event at subcellular site 1. Ca^{2+} diffusing from this region triggered a second release of Ca^{2+} from an adjacent region (site 2). The Ca^{2+} releasing activity of these two regions was sufficient to elevate background Ca^{2+} (site 3) and trigger the regenerative release of Ca^{2+} throughout the entire cell resulting in the Ca^{2+} wave (Fig. 7A).

Clearly, Fluo-3 is capable of reporting both elementary and global Ca^{2+} events. However, other indicators are less useful. We have used Oregon Green 488 BAPTA-1 to monitor Ca^{2+} signals (Fig. 7B), but the contrast obtained with this indicator is significantly less than with Fluo-3. The traces in Figure 7B illustrate that it is possible to detect both elementary and global Ca^{2+} signals with Oregon Green 488 BAPTA-1, but the apparent noise is greater. Furthermore, the elementary Ca^{2+} event depicted in Figure 7Bb is much less obvious than that detected by Fluo-3 (Fig. 7Ab).

The least useful indicator was Calcium Orange. With this indicator it was not possible to distinguish any elementary events. Global Ca^{2+} signals could be observed if the photo multiplier gain was increased, but this manoeuvre significantly increased background noise (Fig. 7C). The simplest reason why these indicators vary so much in their ability to detect elementary and global Ca^{2+} signals is due to their significantly different dynamic ranges. Fluo-3 (and Fluo-4), has the largest dynamic range, and thus provides images with the best contrast. The results obtained with Calcium Orange were also compromised in part by the rapid sequestration of this indicator.

The use of two single wavelength Ca^{2+} indicators (i.e. Fluo-3/Fura-Red) can be used to achieve ratiometic Ca^{2+} imaging [15,16], and thus effectively improve the signal-to-noise and dynamic range. However, this method has a number of caveats. Firstly, both Ca^{2+} indicators must have similar rates of photobleaching otherwise the ratio becomes dominated by a single wavelength. In the case of the Fluo-3 and Fura-Red there is a noticeable difference in the rate of photobleaching ($t_{1/2}$ = 143 s and 251 s respectively, Fig. 2, Table 2) and as a result they can only be used to monitor Ca^{2+} signals over comparatively short periods of time [15,16]. Secondly, accurate quantification of the fluorescence ratio requires the exact amount of

each indicator to be known. This can only be achieved with whole cell patch clamping where indicator concentrations are effectively those included in the microelectrode, and there is little compartmentalization or indicator leakage[15,16].

An example of ratiometric Fluo-3/Fura-Red imaging illustrating the advantage of signal detection that it offers is shown in Figure 8. In this example, an elementary Ca^{2+} signal was evoked by stimulating a HeLa cell with a low histamine concentration. When the fluorescence emission from the individual indicators was examined the signal was more apparent in the Fluo-3 response (Fig. 8Ai) than with Fura-Red (Fig. 8Aii). However, a ratio of the fluorescence emission from these indicators (Fig. 8B) resulted in an improved signal over the background noise, and effectively eliminates the apparent photobleaching over the duration of the recording. As a result there was an increased ability to detect small amplitude elevations in Ca^{2+}.

This study describes the in-situ calibration of a number of commonly used fluorescent indicators, and our empirical observations concerning their applicability for detecting various types of Ca^{2+} signal. Clearly, the choice of Ca^{2+} indicator is entirely dependent on the type of experimental investigation. In our principal application, the study of elementary and global Ca^{2+} signals, Fluo-3 proved to be the indicator of choice. This is essentially as a result of a large dynamic range, which provides images with the best contrast. Unfortunately, in our hands, Fluo-3 is prone to photobleaching and some compartmentalization. The former compromises the duration of experiments and the latter decreases image quality. Other Ca^{2+} indicators were more photostable and gave less compartmentalization, but due to their lower dynamic range they are less suitable than Fluo-3 for studying elementary and global Ca^{2+} signals. In particular, the problems associated with compartmentalization, comparatively low apparent Ca^{2+}-binding affinity and dynamic range (Table 3, Fig. 4), made Calcium Orange a poor choice for monitoring such Ca^{2+} signals.

ACKNOWLEDGEMENTS

DT & SCT were supported by the BBSRC, MDB acknowledges the support of the Royal Society. We thank Dr J. McGuigan (Berne, Switzerland) for the manufacture and supply of Ca^{2+} sensitive electrodes.

REFERENCES

1. Berridge MJ. Elementary and global aspects of calcium signalling. *J Physiol* 1997; **499**: 291–306.
2. Berridge MJ, Bootman MD, Lipp P. Calcium – a life and death signal. *Nature* 1998; **395**: 645–648.
3. Bootman MD, Berridge MJ. The elemental principles of calcium signaling. *Cell* 1995; **83**: 675–678.
4. Bootman MD, Berridge MJ, Lipp P. Cooking with calcium: the recipes for composing global signals from elementary events. *Cell* 1997; **91**: 367–373.
5. Haugland RP. Handbook of Fluorescent Probes and Research Biochemicals. Eugene, Oregon, USA: Molecular Probes Inc, 1996.
6. Grynkiewicz G, Poenie M, Tsien RY. A new generation of Ca^{2+} indicators with greatly improved fluorescence properties. *J Biol Chem* 1985; **260**: 3440–3450.
7. Minta A, Kao JPY, Tsien RY. Fluorescent indicators for cytosolic calcium based on rhodamine and fluorescein chromophores. *J Biol Chem* 1989; **264**: 8171–8178.
8. Thomas D, Lipp P, Tovey SC, Berridge MJ, Li W, Tsien RY, Bootman MD. Microscopic properties of elementary Ca^{2+} release sites in nonexcitable cells. *Curr Biol* 2000; **10**: 8–15.
9. Tovey SC, Thomas D, Lipp P, Berridge MJ, Bootman MD. Cytoplasmic and nucleoplasmic calibration of fluo-3 confirms the lack of nucleo-cytoplasmic Ca^{2+} gradients during stimulation of HeLa cells. *J Physiol* 1998; **515P**: 171P.
10. Bers DM. A simple method for the accurate determination of free $[Ca^{2+}]$ In CaEGTA solutions. *Am J Physiol* 1982; **242**: C404–C408.
11. Mcguigan JAS, Luthi D, Buri A. Calcium buffer solutions and how to make them – a do it yourself guide. *Can J Physiol Pharmacol* 1991; **69**: 1733–1749.
12. Al-Mohanna FA, Caddy KW, Bolsover SR. The nucleus is insulated from large cytosolic calcium ion changes. *Nature* 1994; **367**: 745–750.
13. Bootman MD, Thomas D, Tovey SC, Berridge MJ, Lipp P. Nuclear calcium signalling. *Cell Mol Life Sci* 2000; **57**: 371–378.
14. Bootman MD, Berridge MJ. Subcellular Ca^{2+} signals underlying waves and graded responses in HeLa cells. *Curr Biol* 1996; **6**: 855–865.
15. Lipp P, Niggli E. Ratiometric confocal Ca^{2+} measurements with visible wavelength indicators in isolated cardiac myocytes. *Cell Calcium* 1993; **14**: 359–372.
16. Lipp P, Lüscher C, Niggli E. Photolysis of caged compounds characterized by ratiometric confocal microscopy: a new approach to measure and homogeneously control the calcium concentration in cardiac myocytes. *Cell Calcium* 1996; **18**: 255–266.